J. Fluid Mech. (1990), *vol.* 212, *pp.* 289–308
Printed in Great Britain

Extended Stokes series: laminar flow through a heated horizontal pipe

By MILTON VAN DYKE
Department of Mechanical Engineering, Stanford University, Stanford, CA 94305, USA

(Received 19 May 1989)

Morton's series for fully developed laminar flow through a uniformly heated horizontal pipe is simplified by assuming high Prandtl number, and then extended by computer to 31 terms in powers of a parameter that is the product of the Prandtl, Rayleigh, and Reynolds numbers. As in the analogous problems, treated previously, of flow through a loosely coiled pipe and a slowly rotating pipe, convergence is limited by a conjugate pair of square-root singularities on the imaginary axis. For the global heat flux, an Euler transformation and extraction of the nearest singularity at infinity yield an approximation in good agreement with existing experiment and numerical solution. The Nusselt number is found to grow asymptotically as the $\frac{2}{15}$-power of the parameter, whereas boundary-layer analyses have suggested a $\frac{1}{5}$-power.

1. Introduction

It is easier to calculate external than internal flows when the viscosity is great, but harder when it is small. At a low Reynolds or Rayleigh number R the Stokes linearization provides a basis for successive approximations to internal flows; but it fails for external flows, as exemplified by the paradoxes of Stokes and Whitehead. At the other extreme of high R, boundary layers arise in either geometry; but an external boundary layer is simpler because it traverses the body only once and therefore matches with an outer irrotational flow that be calculated either beforehand in a forced stream or subsequently in a free convection. An internal boundary layer, on the other hand, recirculates endlessly; its interaction with the core is therefore so intimate that the two matching flows must be calculated simultaneously.

For internal flow, the two limits of high and low viscosity were first considered concurrently by Batchelor (1954), treating free convection in the air space between two vertical walls at different temperatures. He began by considering what we call here the Stokes series – an expansion in powers of the Rayleigh number Ra (his A). He estimated that the series would provide a good approximation only for Ra less than about 1000, which was below his region of interest. Then, after analysing the very tall cavity at arbitrary Ra, he turned to the boundary-layer approximation for Ra tending to infinity. He reasoned that the core is isothermal with a constant vorticity whose value is found by matching with the boundary layer. However, various experiments, and several analyses starting with the boundary-layer analysis of Gill (1966), suggest instead a relatively stagnant core with horizontally stratified temperature increasing vertically. This is an example of the fact that recirculating internal boundary layers are neither so simple nor so well understood as external boundary layers.

The utility of the Stokes series has been transformed by the advent of the computer. Batchelor remarked that only the first few terms of his series could be determined numerically without excessive labour; but now – particularly in simpler

geometry – we can compute dozens or even hundreds of terms. From those we can estimate accurately the radius of convergence, and then attempt to extend the range of utility by analytic continuation. The ultimate achievement is to extract from the Stokes series for small R the boundary-layer solution for R tending to infinity.

We first carried out that program successfully for the model problem of the drag of a sphere in linearized Oseen flow (Van Dyke 1970); and we apply it now to the heat transfer in laminar flow through a heated horizontal pipe. That flow is of practical interest because buoyancy induces a secondary motion that may increase the laminar heat transfer by more than a factor of five. The motion was first studied as a perturbation of the classical solution of Nusselt (1910) for fully developed flow through a horizontal pipe by Morton (1959) and independently by Hanratty (unpublished; see Apostolakis 1957).

Subsequent investigators have turned instead to boundary-layer and finite-difference methods, arguing – like Batchelor – that Morton's perturbation solution is accurate only for changes in heat transfer that are small compared with those of practical interest. Our objective here is to remove that limitation by extending the series to high order by computer, analysing its coefficients, and recasting it to be valid over the entire range of physical interest.

Trefethen (1957) has observed that the heated pipe provides one of three analogous situations in which an additional force superimposes upon rectilinear Poiseuille flow a double-spiral secondary motion. The other two are the coiled pipe, first analysed as a perturbation of Poiseuille flow by Dean (1928), and the pipe rotating about a perpendicular axis, treated in a similar way by Barua (1954). Those two series solutions have previously been extended by computer, with controversial results.

The author (Van Dyke 1978) extended Dean's four-term series for the loosely coiled pipe to 24 terms in powers of what is now known as the Dean number. Although he found the result limited by a modest radius of convergence, he claimed to have recast it to be valid for arbitrarily large Dean number. Indeed, he extracted the asymptotic result that the friction ratio eventually increases as the $\frac{1}{4}$-power of the Dean number. Unfortunately, that conclusion is in disagreement with four separate boundary-layer analysis, all of which predict a $\frac{1}{2}$-power. Furthermore, the results fall eventually well below all existing numerical results and all experiments.

Similarly, Mansour (1985) expanded the flow through a slowly rotating pipe to 34 terms in powers of a single combined similarity parameter that he introduced. Recasting the resulting series for the friction ratio, he predicted that it will grow asymptotically as the $\frac{1}{8}$-power of his similarity parameter. However, two different boundary-layer analyses predict instead a $\frac{1}{4}$-power.

These discrepancies have naturally cast doubt on the trustworthiness of the process, proposed in those two papers, of numerical analytic continuation far beyond the original radius of convergence. Furthermore, Hunter (1987) has issued a warning, bolstered by model functions, that 'it may be difficult to make an accurate estimate of the unknown limiting behaviour of some function $P(R)$ as $R \to \infty$ from the Euler transformed series' (the Euler transformation being an essential part of the process). These uncertainties discouraged us from completing our analysis of the heated pipe, the bulk of which was carried out ten years ago.

The outlook has changed significantly, however, with the appearance of careful new experiments in a coiled pipe by Ramshankar & Sreenivasan (1988). From a detailed review of previous experiments, they conclude that none of the existing data satisfy the conditions demanded by the computer-extended theory: a disturbance level of the incoming flow low enough to maintain laminar flow to relatively high

Reynolds numbers, a loose coil whose cross-section radius is less than 0.03 of the coiling radius, nearly circular cross-section, adequate length to achieve fully developed flow, and values of Dean number greater than 500. Ramshankar & Sreenivasan managed to match those requirements reasonably well, and measured friction factors that fall below the boundary-layer predictions, and lie close to the $\frac{1}{4}$-power variation deduced from the computer extension. They concede, however, that the 'paradox' is not yet completely resolved satisfactorily, because a discrepancy remains with trustworthy finite-difference computations that satisfy precisely the conditions for series extension (Collins & Dennis 1975; Dennis 1980; Daskopoulos & Lenhoff 1989). Nevertheless, Ramshankar & Sreenivasan's results for the coiled pipe have encouraged us to take up again our interrupted analysis of the analogous heated-pipe problem; and we are delighted to find that, although our results again disagree with several approximate boundary-layer analyses, they are in close accord with both experimental and finite-difference results.

2. Reduction of Morton's problem

We consider Morton's problem of fully developed steady laminar flow through a horizontal pipe of radius a whose wall is heated uniformly. We neglect dissipation, and the pressure term in the energy equation, and variations of density except in the buoyancy force, and take the kinematic viscosity ν and thermal diffusivity κ as constants. We introduce cylindrical coordinates (r, ϕ, x) with x increasing in the streamwise direction and ϕ measured from the upward vertical.

We mainly follow Morton's notation. A constant temperature gradient τ is maintained in the axial direction; and in full developed flow the pressure has a constant (negative) gradient γ. Then the velocity components u, v, w in the fluid and the temperature decrement $\tau x - T$ are functions of r and ϕ only. The continuity equation can be satisfied by introducing a Stokes stream function ψ for the crossflow. Morton introduces dimensionless variables by referring r to a, u, v, and w to ν/a and hence ψ to ν, and $\tau x - T$ to aPr, where the Prandtl number is $Pr = \nu/\kappa$. The problem then depends upon three dimensionless parameters, the Prandtl number Pr, Rayleigh number Ra, and Reynolds number Re (Morton's σ, A, and B), where

$$Ra = \frac{\beta g \tau a^4}{\kappa \nu}, \quad Re = \frac{(-\gamma) a^3}{4\rho\nu^2}. \tag{2.1}$$

Here β is the coefficient of thermal expansion and g the acceleration due to gravity. Re is what Woods & Morris (1974) aptly call the *pseudo Reynolds number* – based on the radius and the maximum speed that would be produced by the pressure gradient in the absence of heating.

We modify Morton's variables in order to clarify the dependence of the problem on the parameters Pr, Ra, and Re. We refer ψ to κ rather than ν, multiply Morton's dimensionless temperature difference and axial velocity w by the Reynolds number Re, and then subtract the parabolic Poiseuille velocity profile from w and divide the remainder by Pr. Thus we express the original dimensional variables in terms of new (barred) variables as

$$\left.\begin{aligned} \psi &= \kappa \bar{\psi}(\bar{r}, \phi), \quad r = a\bar{r}, \\ w &= \frac{\nu}{a} Re \left[(1 - \bar{r}^2) + \frac{1}{Pr} \bar{w}(\bar{r}, \phi) \right], \\ T &= \tau \bar{x} - \tau a \, Pr \, Re \, \theta(\bar{r}, \phi). \end{aligned}\right\} \tag{2.2}$$

Then the vorticity equation, axial-momentum equation, and energy equation reduce, with the overbars dropped, to

$$\nabla^4\psi+\frac{1}{Pr}\frac{1}{r}\left(\frac{\partial\psi}{\partial r}\frac{\partial}{\partial\phi}-\frac{\partial\psi}{\partial\phi}\frac{\partial}{\partial r}\right)\nabla^2\psi=(Pr\,Ra\,Re)\left(\frac{\partial\theta}{\partial r}\sin\phi+\frac{1}{r}\frac{\partial\theta}{\partial\phi}\cos\phi\right), \tag{2.3}$$

$$\nabla^2 w+2\frac{\partial\psi}{\partial\phi}+\frac{1}{Pr}\frac{1}{r}\left(\frac{\partial\psi}{\partial r}\frac{\partial w}{\partial\phi}-\frac{\partial\psi}{\partial\phi}\frac{\partial w}{\partial r}\right)=0, \tag{2.4}$$

$$\nabla^2\theta+\frac{1}{r}\left(\frac{\partial\psi}{\partial r}\frac{\partial\theta}{\partial\phi}-\frac{\partial\psi}{\partial\phi}\frac{\partial\theta}{\partial r}\right)+(1-r^2)+\frac{1}{Pr}w=0. \tag{2.5}$$

These correspond to Morton's equations (4), (5), (6); but our modified variables have the advantage of showing that the problem depends not upon Pr, Ra, and Re separately, but only upon the Prandtl number Pr and the combination

$$\epsilon=Pr\,Ra\,Re=\frac{\beta g\tau(-\gamma)a^7}{4\rho\nu^2\kappa^2}. \tag{2.6}$$

This correlation was first observed by Anderson (1970), whose parameter $X^{\frac{1}{2}}$ is the product of his Grashof, Nusselt, and Prandtl numbers, and equal to half our ϵ. It has been independently rediscovered by Cheng, Hwang & Akiyama (1972) and Woods & Morris (1980).

Finally, we simplify the problem further, reducing the original three parameters to this single combination, by neglecting terms multiplied by $1/Pr$. This approximation would seem entirely satisfactory for oil, with Pr of order one thousand, and perhaps acceptable even for cool water, with Pr of order five. In fact, however, the effects of finite Prandtl number appear to be small and compensatory. This is suggested by Morton's second approximation for the Nusselt number Nu:

$$Nu=6\left[1+(0.0586-0.0852Pr+0.2686Pr^2)\left(\frac{Ra\,Re}{4608}\right)^2+\ldots\right]. \tag{2.7}$$

Here the error incurred by neglecting all but the highest powers of Pr is less than 12% of the correction when Pr is greater than 0.6, which includes gases such as air. Thus we seek to solve the simplified equations

$$\left.\begin{aligned}&\nabla^4\psi=\epsilon\left(\sin\phi\frac{\partial\theta}{\partial r}+\frac{\cos\phi}{r}\frac{\partial\theta}{\partial\phi}\right),\\&\nabla^2 w+2\frac{\partial\psi}{\partial\phi}=0,\\&\nabla^2\theta+\frac{1}{r}\left(\frac{\partial\psi}{\partial r}\frac{\partial\theta}{\partial\phi}-\frac{\partial\psi}{\partial\phi}\frac{\partial\theta}{\partial r}\right)+(1-r^2)=0.\end{aligned}\right\} \tag{2.8}$$

Our approximation of large Prandtl number has rendered the first two equations linear, and uncoupled the second from the other two. We can therefore solve for the crossflow and temperature fields alone and, if desired, subsequently calculate the axial velocity, which according to (2.2) differs from the parabolic Poiseuille profile only by small terms of order $1/Pr$.

The boundary conditions on ψ and w require that the three components of velocity vanish at the wall:

$$\frac{\partial\psi}{\partial r}=\frac{\partial\psi}{\partial\phi}=w=0\quad\text{at}\quad r=1. \tag{2.9}$$

Two different boundary conditions on temperature are found in the literature. Morton (1959) interprets the 'uniformly heated' of his title to mean that the wall temperature increases linearly downstream, but is constant around the circumference at any station. He argues that 'pipes will usually have reasonably thick walls of material with thermal conductivity much higher than that of the fluid, and so there will be little variation in wall temperature round the pipe girth.' Thus his wall temperature is simply τx, independent of ϕ, and the local heat flux then varies with ϕ, being slightly greater at the bottom than the top. Thus his boundary condition is

$$\theta = 0 \quad \text{at} \quad r = 1. \tag{2.10}$$

Most subsequent investigators have adopted this condition, which Morcos & Bergles (1975) call that of *infinite conductivity*.

On the other hand, Anderson interprets 'uniformly heated' strictly; the local heat flux is taken to be constant everywhere on the wall, and the temperature of the wall then varies with ϕ, being slightly higher at the bottom than the top. Thus his boundary condition is that of *zero conductivity*,

$$\frac{\partial \theta}{\partial r} = \text{const.} \quad \text{at} \quad r = 1. \tag{2.11}$$

He takes τx to be the bulk (mixed-mean, mixing-cup) temperature

3. Perturbation solution

Morton (1959) sought an approximation for slight heating by expanding in powers of the Rayleigh number Ra, with the Prandtl and Reynolds numbers as parameters. However, he observed that Ra and Re appeared only as a product, so he effectively expanded in powers of $RaRe$, with coefficients that are polynomials in Pr of continually increasing order. Hence he computed (to second order) a double power series in $RaRe$ and Pr.

Anderson (1970) delegated the mounting algebra to the computer and, for the boundary condition (2.11) of strictly uniform heat transfer, calculated seven terms of the single series in powers of our ϵ (his $2X^{\frac{1}{2}}$). We here extend the computation further for both boundary conditions.

We substitute into our simplified equations (2.8) the expansions

$$\left.\begin{aligned} \theta &= \theta_0 + \epsilon\theta_1 + \epsilon^2\theta_2 + \ldots, \\ \psi &= \quad\ \epsilon\psi_1 + \epsilon^2\psi_2 + \ldots, \\ w &= \quad\ \epsilon w_1 + \epsilon^2 w_2 + \ldots. \end{aligned}\right\} \tag{3.1}$$

Then equating like powers of ϵ gives for θ_0 the equation

$$\nabla^2\theta_0 \equiv \left(\frac{\partial^2}{\partial r^2} + \frac{1}{r}\frac{\partial}{\partial r} + \frac{1}{r^2}\frac{\partial^2}{\partial \phi^2}\right)\theta_0 = -(1-r^2). \tag{3.2}$$

Integrating and imposing Morton's condition (2.10) yields

$$\theta_0 = \tfrac{1}{16}(3 - 4r^2 + r^4). \tag{3.3}$$

On the other hand, Anderson requires that the bulk temperature be the basic τx, so the average over the cross-section of this increment, weighted by the parabolic

Poiseuille velocity, must vanish. This lowers the constant of integration, giving instead

$$\theta_0 = \tfrac{1}{16}(\tfrac{7}{6} - 4r^2 + r^4). \tag{3.4}$$

Either of these is the classical result of Nusselt (1910) for flow in the absence of buoyancy. It gives the value $-\frac{1}{4}$ for the constant in Anderson's boundary condition (2.11), and all higher-order terms must satisfy $\partial\theta_n/\partial r = 0$ at the walls. Then the equations for ψ_1 and w_1 are readily integrated to give

$$\left.\begin{aligned} \psi_1 &= -\tfrac{1}{4608} r(1-r^2)^2(10-r^2)\sin\phi, \\ w_1 &= -\tfrac{1}{184\,320} r(1-r^2)(49-51r^2+19r^4-r^6)\cos\phi. \end{aligned}\right\} \tag{3.5}$$

We shall consider the axial velocity no further, because it differs from the Poiseuille flow by only terms of order $1/Pr$.

In the second cycle, the differential equation for θ_1 is

$$\nabla^2\theta_1 = \tfrac{1}{18\,432} r(20-52r^2+45r^4-14r^6+r^8)\cos\phi. \tag{3.6}$$

For Morton's boundary condition of infinite conductivity, the solution is

$$\theta_1 = -\tfrac{1}{4\,423\,680} r(265-600r^2+520r^4-225r^6+42r^8-2r^{10})\cos\phi, \tag{3.7}$$

whereas for Anderson's condition (2.11) of zero conductivity, the first coefficient 265 is replaced by 419. Then under either condition the equation for ψ_2 is integrated to give

$$\psi_2 = \tfrac{1}{2800(4608)^2} r^2(1-r^2)^2(10\,518-4614r^2+1254r^4-158r^6+5r^8)\sin 2\phi. \tag{3.8}$$

In the third cycle, integrating the equation for θ_2 for infinite conductivity gives

$$\begin{aligned} \theta_2 = \tfrac{1}{14\,700(4608)^3}[&(-9\,070\,460+46\,746\,000r^2-102\,003\,300r^4+123\,362\,400r^6 \\ &-91\,000\,350r^8+42\,283\,080r^{10}-12\,118\,680r^{12}+1\,942\,920r^{14} \\ &-145\,530r^{16}+3920r^{18})+(7\,594\,290r^2-23\,762\,088r^4+32\,275\,404r^6 \\ &-25\,016\,040r^8+11\,779\,110r^{10}-3\,383\,856r^{12}+552\,573r^{14}-40\,464r^{16} \\ &+1071r^{18})\cos 2\phi]. \end{aligned} \tag{3.9}$$

For zero conductivity, the first five coefficients inside the first parentheses are replaced by $-130\,075\,498/11$, $73\,911\,600$, $-130\,527\,180$, $134\,228\,640$, and $-91\,679\,490$, and the first four coefficients in the second parenthesis by $-7\,140\,276$, $-476\,168$, $24\,125\,724$, and $-24\,472\,728$. All these results for Morton's boundary condition agree with those of Morton himself except for the last coefficient in (3.7), the first two in the second parenthesis in (3.9), and the sign of the sixth; but our results are confirmed by the later calculations of Iqbal & Stachiewicz (1966).

We want to analyse a global quantity of practical interest. Morton considers both the volume flux and the heat flux. However, the axial velocity is unaltered by buoyancy in our approximation of high Prandtl number. We therefore examine henceforth the global heat flux, as given by the Nusselt number Nu.

The Nusselt number is by definition proportional to the heat flux into the fluid – which is also unaltered by buoyancy in our analysis – and inversely proportional to the difference between the mean temperatures of the wall and of the fluid. In Morton's problem the wall temperature is τx, so Nu is proportional to the average across the pipe of the temperature difference θ. If the unweighted mean is used, integrating (3.3) gives the classical value $Nu_0 = 6$. Then the ratio of this to the Nusselt number including buoyancy is given by

$$\frac{Nu_0}{Nu} = \frac{12}{\pi}\int_{r=0}^{1}\int_{\phi=0}^{2\pi} \theta r\,\mathrm{d}\phi\,\mathrm{d}r = 1 - \frac{72\,143}{268\,800}\left(\frac{\epsilon}{4608}\right)^2 + \ldots. \tag{3.10}$$

This agrees with Morton's result (2.7) for large Prandtl number.

To compare with experiment, however, one must use the bulk temperature – the average weighted with respect to the axial velocity (Goldstein 1938, p. 618). Using the parabolic velocity profile gives $Nu_0 = \frac{48}{11}$ in the classical case, and with the inclusion of buoyancy,

$$\frac{Nu_0}{Nu} = \frac{384}{11}\frac{1}{2\pi}\int_{r=0}^{1}\int_{\phi=0}^{2\pi}(1-r^2)\theta r\,\mathrm{d}\phi\,\mathrm{d}r = 1-\frac{45187}{135520}\left(\frac{\epsilon}{4608}\right)^2+\ldots. \tag{3.11}$$

This agrees with the large-Pr limit of equation (4) of Mori *et al.* (1966) and equation (36) of Iqbal & Stachiewicz (1966), who recast Morton's result (2.7) into bulk-temperature form.

In Anderson's version of the problem, the bulk temperature is τx, so Nu is proportional to the average value of the temperature difference θ at the wall. Hence the ratio of Nusselt numbers is given by

$$\frac{Nu_0}{Nu} = -\frac{96}{11}\frac{1}{2\pi}\int_{\phi=0}^{2\pi}\theta(1,\phi)\,\mathrm{d}\phi = 1-\frac{1590871}{2032800}\left(\frac{\epsilon}{4608}\right)^2+\ldots. \tag{3.12}$$

This agrees with the result (4.1) of Anderson (1970) that is quoted in the next section.

We shall eventually invert these expressions to obtain the 'direct' ratio Nu/Nu_0 that is normally considered in the literature. However, we retain this 'reciprocal' ratio throughout our analysis in the expectation that it is better behaved, because it ranges only between zero and one.

4. Computer-extended series

The results summarized above represent the present limit of hand computation. Beyond that, Anderson, using an ingenious 'superscript summation convention' to organize the work on a computer (Reynolds & Potter 1967), calculated five terms with the effects of flow expansion included, and seven terms in the Boussinesq approximation adopted here. Thus he added two terms to the series (3.12) for the reciprocal ratio of Nusselt numbers:

$$\frac{Nu_0}{Nu} = 1-1.4742\times10^{-7}(\tfrac{1}{2}\epsilon)^2+1.6393\times10^{-13}(\tfrac{1}{2}\epsilon)^4-2.4749\times10^{-19}(\tfrac{1}{2}\epsilon)^6+\ldots. \tag{4.1}$$

We have undertaken to extend this series solution considerably farther by computer, with the aim of analysing its coefficients and thereby extending its utility. We first rewrite the series (3.1) for θ as

$$\theta(r,\phi;\epsilon) = \sum_{n=0}^{\infty}\left(\frac{\epsilon}{S}\right)^n\theta_n(r,\phi). \tag{4.2}$$

and similarly for ψ and w. Here S is a scale factor to be chosen so as to avoid overflow or underflow. Results such as (3.12) suggest that it should be of the order of 4608. Then substituting into the governing equations (2.8) and equating like powers of ϵ yields an equation for the nth term in the series for ψ:

$$\nabla^4\psi_n = S\left(\sin\phi\frac{\partial\theta_{n-1}}{\partial r}+\frac{\cos\phi}{r}\frac{\partial\theta_{n-1}}{\partial\phi}\right), \tag{4.3}$$

together with a similar equation for $\nabla^2 w_n$, and one for $\nabla^2\theta_n$ that involves a convolution summation because of the quadratic nonlinearity.

Inspection of (3.3) or (3.4), (3.7), and (3.9) indicates that the functions θ_n have the form

$$\theta_n(r,\phi) = \sum_{j=1}^{[(n+2)/2]} \sum_{k=1}^{[(7n+6)/2]} C_{njk}\, r^{2k-1-p} \cos(2j-1-p)\,\phi. \tag{4.4}$$

Here the square brackets mean the greatest integer; and p is a 'parity number', equal to zero when n is odd and unity when n is even. We have analogous forms for $\nabla^2\theta_n$, ψ_n, $\nabla^4\psi_n$, w_n, and $\nabla^2 w_n$. At the nth cycle of the solution, we substitute the expression (4.4) for θ_n into the differential equation (4.3), replace products of sines and cosines by sums and differences, and then run through the double summation, assigning coefficients of like powers of r and sines of like argument to the matrix of coefficients in the expression for $\nabla^4\psi_n$. Next, quadratures, and imposition of boundary conditions, yield the corresponding matrix for ψ_n itself. We then increase n by one and carry out a similar process for $\nabla^2\theta_{n+1}$, which involves a five-fold summation, and finally for θ_{n+1}. After calculating the coefficient of the Nusselt number (if n is even), we start a new cycle.

We have written a FORTRAN program of some 280 lines that carries out this iterative process for the boundary condition on temperature of either zero or infinite conductivity of the pipe. The program consists mostly of nested Do-loops; and the bulk of the computation is devoted to Do-loops nested five deep to evaluate the nonlinear right-hand side of the equation for $\nabla^2\theta_n$. Consequently, the computing time required is found to increase as the sixth power of the number of terms.

We have eventually carried the solution to 31 terms in quadruple-precision arithmetic for both temperature conditions. Comparison with a double-precision run† suggests that we have lost fewer than 15 significant figures at the end, so our results are correct to more than 16 figures. That is the number we have retained in all subsequent analysis (though of course we quote here mostly truncated results).

5. Analysis of the coefficients

Only even powers of ϵ contribute to the series (4.1) for the reciprocal ratio of Nusselt numbers, which has the form

$$\frac{Nu_0}{Nu} = 1 + \sum_{n=1}^{\infty} a_n \left(\frac{\epsilon}{S}\right)^{2n}. \tag{5.1}$$

Table 1 lists the first 16 coefficients a_n, computed with the scale factor $S = 1152$, for the three cases outlined above. These are Anderson's series (4.1) for circumferentially constant heat transfer with the Nusselt number based on the bulk fluid temperature, the reciprocal (3.10) of Morton's series for circumferentially constant temperature with the Nusselt number based on mean fluid temperature, and the series (3.11) obtained by recasting Morton's solution into bulk-temperature form.

In all three cases, just as in the two related problems of the coiled and the rotating pipe, the signs of the coefficients alternate regularly, indicating that the nearest singularity lies on the negative axis of ϵ^2. Hence there is a complex-conjugate pair of singularities on the imaginary axis of ϵ itself. For Anderson's series, the coefficients are seen to decrease only slowly in magnitude, which suggests that the series converges for ϵ slightly greater than 1152. In Morton's two versions, the radius of

† We have since learned from Hideaki Takagi (unpublished communication) that a better way of estimating the loss of accuracy due to accumulated round-off error is to compare two runs of the highest available precision, carried out with different values of the scale factor S that are not in the ratio of a power of 2.

n	Zero conductivity, bulk temperature	Infinite conductivity, mean temperature	Infinite conductivity, bulk temperature
0	1.00000 00000 00000	1.0000 00000 00000	1.0000 00000 00000
1	$-4.8912\ 55288\ 27233 \times 10^{-2}$	$-1.6774\ 32105\ 65476 \times 10^{-2}$	$-2.0839\ 63621\ 60567 \times 10^{-2}$
2	$1.8045\ 56408\ 64384 \times 10^{-2}$	$2.3809\ 08442\ 14119 \times 10^{-3}$	$3.0050\ 84964\ 49532 \times 10^{-3}$
3	$-9.0396\ 05176\ 70404 \times 10^{-3}$	$-4.6368\ 33322\ 83201 \times 10^{-4}$	$-5.8891\ 26581\ 12572 \times 10^{-4}$
4	$5.2086\ 79836\ 33005 \times 10^{-3}$	$1.0418\ 46910\ 56412 \times 10^{-4}$	$1.3276\ 03670\ 23338 \times 10^{-4}$
5	$-3.2548\ 78205\ 26549 \times 10^{-3}$	$-2.5418\ 43436\ 66901 \times 10^{-5}$	$-3.2455\ 95771\ 92275 \times 10^{-5}$
6	$2.1448\ 38773\ 59787 \times 10^{-3}$	$6.5435\ 11168\ 97357 \times 10^{-6}$	$8.3666\ 32151\ 14730 \times 10^{-6}$
7	$-1.4673\ 44090\ 31272 \times 10^{-3}$	$-1.7494\ 40926\ 79874 \times 10^{-6}$	$-2.2390\ 63181\ 77177 \times 10^{-6}$
8	$1.0322\ 43172\ 71277 \times 10^{-3}$	$4.8105\ 24495\ 22302 \times 10^{-7}$	$6.1614\ 26480\ 87002 \times 10^{-7}$
9	$-7.4199\ 31000\ 71946 \times 10^{-4}$	$-1.3518\ 05124\ 98275 \times 10^{-7}$	$-1.7324\ 22883\ 80411 \times 10^{-7}$
10	$5.4260\ 01716\ 78194 \times 10^{-4}$	$3.8649\ 16597\ 19641 \times 10^{-8}$	$4.9554\ 27731\ 71237 \times 10^{-8}$
11	$-4.0238\ 80011\ 61351 \times 10^{-4}$	$-1.1206\ 80136\ 61777 \times 10^{-8}$	$-1.4374\ 32840\ 01925 \times 10^{-8}$
12	$3.0190\ 29525\ 22571 \times 10^{-4}$	$3.2877\ 83455\ 24059 \times 10^{-9}$	$4.2183\ 89197\ 49774 \times 10^{-9}$
13	$-2.2874\ 91410\ 54525 \times 10^{-4}$	$-9.7411\ 88105\ 26416 \times 10^{-10}$	$-1.2501\ 78050\ 42213 \times 10^{-9}$
14	$1.7478\ 51981\ 49147 \times 10^{-4}$	$2.9106\ 32407\ 85380 \times 10^{-10}$	$3.7363\ 47256\ 62418 \times 10^{-10}$
15	$-1.3452\ 74411\ 24656 \times 10^{-4}$	$-8.7606\ 17556\ 76363 \times 10^{-11}$	$-1.1248\ 15406\ 27376 \times 10^{-10}$

TABLE 1. Coefficients a_n of series (5.1) with $S = 1152$.

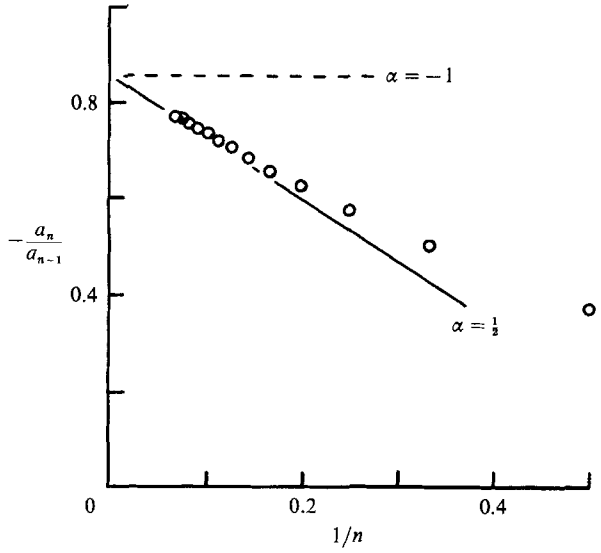

FIGURE 1. Domb–Sykes plot for extended Anderson series (5.1).

convergence appears to be somewhat greater than that. Because all three solutions have very similar structure, we analyse only Anderson's in detail.

We can estimate the radius of convergence, and at the same time the nature of the nearest singularity, by forming a Domb–Sykes plot – a graph of the ratios $-a_n/a_{n-1}$ of successive coefficients versus $1/n$. Figure 1 shows that the plot is quickly becoming straight as n increases. This indicates that the coefficients are approaching those of an algebraic singularity, a multiple of $[\mathscr{R}^2 + (\epsilon/S)^2]^\alpha$, for which

$$\frac{a_n}{a_{n-1}} = -\frac{1}{\mathscr{R}^2}\left(1 - \frac{1+\alpha}{n}\right). \tag{5.2}$$

The linear extrapolation shown in figure 1 corresponds to $\alpha = \frac{1}{2}$; and a square root was the form of nearest singularity found also for the coiled and the rotating pipes. (For comparison, a simple pole would correspond to an exponent $\alpha = -1$ and hence to the dashed horizontal line.)

The vertical intercept shown corresponds to a radius of convergence of $(\epsilon/1152) = \mathscr{R} = 1.08$. Careful graphical extrapolation might yield one more significant figure than this; but the much greater accuracy inherent in our coefficients is revealed numerically by fitting higher-order polynomials in powers of $1/n$ through several points. The triangular array of all such extrapolations for the vertical intercept, which is our estimate for $\mathscr{R}^{-2}$, is easily constructed by forming a Neville table (Gaunt & Guttmann 1974). The last few entries are

12 ...	0.85136 86786			
13 ...	0.85136 86716	0.85136 86710		
14 ...	0.85136 86711	0.85136 86711	0.85136 86711	
15 ...	0.85136 86718	0.85136 86720	0.85136 86721	0.85136 86722

The last entry, for example, is the vertical intercept found by fitting a 14th-degree polynomial through all 15 ratios of coefficients. This is a remarkably well-behaved Neville table.

The corresponding table for the exponent α shows values between 0.5000000 and 0.5000007 in the fourth column from the end, and either 0.5000000 or 0.5000001 in subsequent columns, so there is little doubt that the singularity is precisely a square root. Assuming that to be true, we can form a more accurate 'biased' Neville table for $\mathscr{R}^{-2}$, which ends with

12 ...	0.8513 68671 353			
13 ...	0.8513 68671 312	0.8513 68671 309		
14 ...	0.8513 68671 292	0.8513 68671 290	0.8513 68671 289	
15 ...	0.8513 68671 292	0.8513 68671 292	0.8513 68671 293	0.8513 68671 293

Here we can confidently estimate that $\mathscr{R}^{-2} = 0.85136\,86713$, so that $\mathscr{R} = 1.0837\,80088$ to at least ten significant figures. The series therefore converges for ϵ less than $\epsilon_0 = 1248.514661$. From his four terms, Anderson (1970) estimated the radius of convergence for his parameter $X = (\frac{1}{2}\epsilon)^2$ as less than 5.0×10^5, which we here refine to $3.897\ldots \times 10^5$.

We shall see that at this limit of convergence the effects of buoyancy have increased the Nusselt number by less than 4.3%. Experiments show that the practical range of laminar flow extends much further, with Nusselt number increasing by as much as a factor of four or five. We must therefore greatly extend the range of validity of our solution in order to make it useful.

6. Improvement of convergence

We have tried to extract the square-root singularity by forming the new series for $[\mathscr{R}^2 + (\epsilon/S)^2]^{-\frac{1}{2}}(Nu_0/Nu)$; but then a new Domb–Sykes plot shows unmistakably an inverse square-root singularity at the same location. This means that the nearest singularity is not a multiplicative square root but an additive one, preceded by a constant, and therefore cannot be removed in this way.

Instead, because a singularity on the negative axis of ϵ^2 is of no physical

n	b_n	c_n	d_n
0	1.0000 00000	1.0000 00000	1.0000 00000
1	$-5.7451\,67109\times10^{-2}$	$9.2149\,95573\times10^{-3}$	$5.7451\,67110\times10^{-2}$
2	$-3.2555\,35253\times10^{-2}$	$-8.2990\,83853\times10^{-4}$	$3.5856\,04705\times10^{-2}$
3	$-2.2307\,64569\times10^{-2}$	$-2.0269\,01444\times10^{-3}$	$2.6237\,99492\times10^{-2}$
4	$-1.6794\,36589\times10^{-2}$	$-2.0676\,76396\times10^{-3}$	$2.0750\,70032\times10^{-2}$
5	$-1.3378\,22868\times10^{-2}$	$-1.8940\,18980\times10^{-3}$	$1.7189\,30664\times10^{-2}$
6	$-1.1066\,51235\times10^{-2}$	$-1.6933\,24040\times10^{-3}$	$1.4685\,70217\times10^{-2}$
7	$-9.4046\,55624\times10^{-3}$	$-1.5087\,97888\times10^{-3}$	$1.2827\,00748\times10^{-2}$
8	$-8.1560\,56319\times10^{-3}$	$-1.3486\,47477\times10^{-3}$	$1.1391\,16783\times10^{-2}$
9	$-7.1858\,19330\times10^{-3}$	$-1.2118\,47892\times10^{-3}$	$1.0247\,89920\times10^{-2}$
10	$-6.4115\,99001\times10^{-3}$	$-1.0951\,96919\times10^{-3}$	$9.3156\,19745\times10^{-3}$
11	$-5.7803\,78566\times10^{-3}$	$-9.9535\,69176\times10^{-4}$	$8.5405\,90317\times10^{-3}$
12	$-5.2565\,33624\times10^{-3}$	$-9.0940\,64698\times10^{-4}$	$7.8859\,46068\times10^{-3}$
13	$-4.8152\,71581\times10^{-3}$	$-8.3493\,01320\times10^{-4}$	$7.3255\,42066\times10^{-3}$
14	$-4.4388\,24350\times10^{-3}$	$-7.6997\,11326\times10^{-4}$	$6.8403\,13248\times10^{-3}$
15	$-4.1141\,36847\times10^{-3}$	$-7.1295\,31645\times10^{-4}$	$6.4160\,25399\times10^{-3}$

TABLE 2. Coefficients after Euler transformation, in series (6.2), (6.4), and (A 7).

significance, we map it away to infinity by applying an Euler transformation, recasting our series (5.1) in powers of the new perturbation parameter

$$\delta = \frac{(\epsilon/S)^2}{\mathscr{R}^2+(\epsilon/S)^2} = \frac{(\epsilon/\epsilon_0)^2}{1+(\epsilon/\epsilon_0)^2}. \tag{6.1}$$

This gives

$$\frac{Nu_0}{Nu} = 1+\sum_{n=1}^{\infty} b_n\,\delta^n = 1-0.5745\delta-0.03256\delta^2-0.02231\delta^3-\ldots. \tag{6.2}$$

We list the new coefficients b_n in table 2. They have fixed signs after the first, which means that the nearest singularity now lies on the positive axis. We anticipate that it lies at $\delta = 1$, corresponding to a singularity at $\epsilon = \infty$. This is confirmed by the new Domb–Sykes plot of figure 2, and more precisely by a Neville table, whose later entries are unity to at least five significant figures. Thus our transformed series converges for all finite ϵ.

At the limit of convergence of the original series, δ is only $\frac{1}{2}$ and our new series (6.2) yields $Nu_0/Nu = 0.9585755$ or $Nu/Nu_0 = 1.0432146$, correct to this many figures. At three times that value of ϵ, however, where the Nusselt number has not yet doubled, our series with $\delta = \frac{9}{10}$ converges so slowly that our 16 terms yield only two-figure accuracy. Our solution needs to be further improved.

The key is clearly to analyse the singularity at $\delta = 1$, to find how the solution is behaving for large ϵ. The Domb–Sykes plot is again becoming straight, indicating a singularity of the form $(1-\delta)^{\beta}$. If the reciprocal ratio Nu_0/Nu is to vanish at large ϵ, that must also be the leading term as $\delta\to1$ (that is, there is no additive constant preceding it). Then the direct ratio Nu/Nu_0 will be singular like $(1-\delta)^{-\beta}$. In terms of the original parameter ϵ this implies, according to (6.1), the asymptotic behaviour

$$\frac{Nu_0}{Nu} \sim \text{const.}\times\epsilon^{-2\beta} \quad \text{or} \quad \frac{Nu}{Nu_0} \sim \text{const.}\times\epsilon^{2\beta} \quad \text{as} \quad \epsilon\to\infty. \tag{6.3}$$

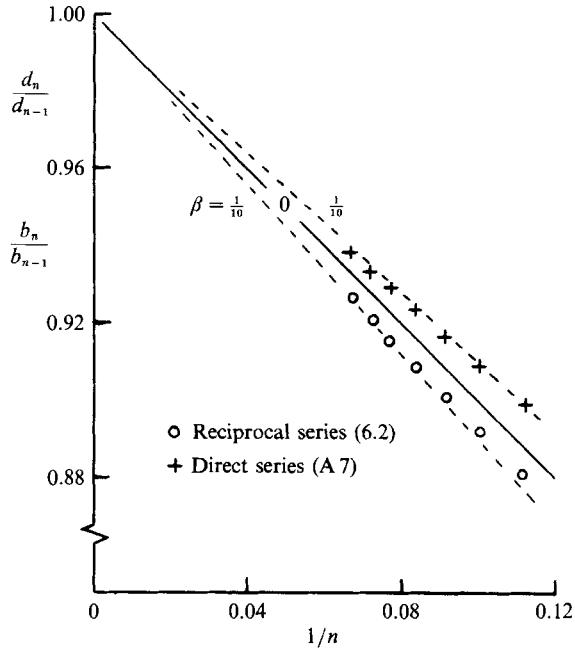

FIGURE 2. Detail of Domb–Sykes plot for Euler-transformed series (6.2) for Nu_0/Nu and its reciprocal (A 7).

We have now, as in the companion problems of the coiled and the rotating pipe, reached a crucial and delicate stage in our analysis. The Domb–Sykes plot of figure 2 shows that the important exponent β is positive (as it should be if Nu is to grow with ϵ) but very small, probably less than $\frac{1}{10}$. We have devoted considerable effort to estimating it reliably. In the Appendix we describe the three techniques that have yielded the most conclusive estimates. These involve examining Padé approximants to the logarithmic derivative of the original series (5.1), calculating the expansion for the logarithmic derivative of the Euler-transformed series (6.2), and comparing the direct and reciprocal series. These indicate that the exponent β is probably 0.067 to two significant figures. Experience leads us to expect a simple rational fraction, and we therefore conclude that $\beta = \frac{1}{15}$.

The leading singularity can then be extracted multiplicatively, which transforms our reciprocal series (6.2) to

$$\frac{Nu_0}{Nu} = (1-\delta)^{\frac{1}{15}}\left[1 + \sum_{n=1}^{\infty} c_n \delta^n\right] = (1-\delta)^{\frac{1}{15}}[1 + 0.00921\delta - \ldots]. \tag{6.4}$$

Table 2 lists the new coefficients c_n. We could now analyse this new series. A Domb–Sykes plot clearly indicates a confluent algebraic singularity at $\delta = 1$, so that the bracket in (6.4) represents a function of the form $(1-k) + k(1-\delta)^{\gamma} + \ldots$. Here the secondary exponent γ is positive, and a Neville table suggests that it may be $\frac{1}{2}$. We have not pursued these details, however, because we see that our result is already sufficiently accurate for practical purposes.

The bracketted series in (6.4) is very close to unity in the range $0 < \delta < 1$ of physical interest. It rises slightly and then falls to 0.97 at $\delta = 1$. Accepting an error

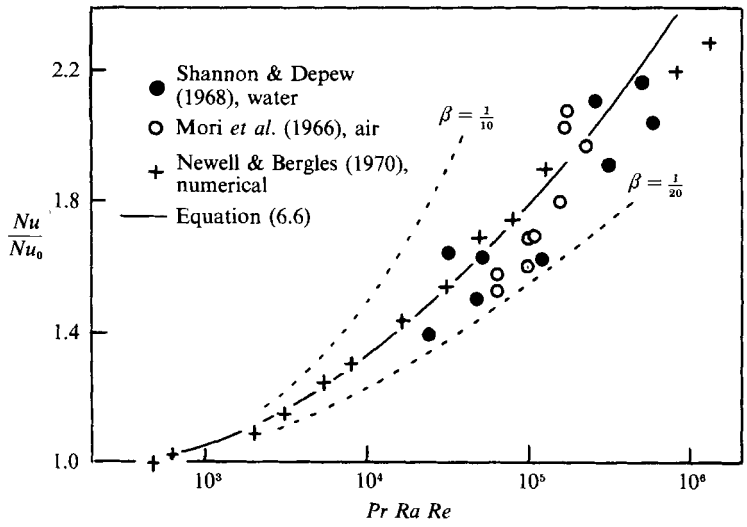

FIGURE 3. Comparison of present theory with experiment and numerical solution.

of not more than a few per cent, we may set it equal to unity. Then (6.4) gives for the direct ratio

$$\frac{Nu}{Nu_0} = (1-\delta)^{-\frac{1}{15}} = \left[1+\left(\frac{\epsilon}{\epsilon_0}\right)^2\right]^{\frac{1}{15}} = \left[1+\left(\frac{Pr\,Ra\,Re}{1249}\right)^2\right]^{\frac{1}{15}}. \tag{6.5}$$

The last result has been expressed in terms of our original product of Prandtl, Rayleigh, and Reynolds numbers, using our radius of convergence truncated to four figures.

For large ϵ, the bracket in (6.4) approaches 0.97, which yields the asymptotic result

$$\frac{Nu}{Nu_0} \sim 0.97(\epsilon/\epsilon_0)^{\frac{2}{15}} = 0.375(Pr\,Ra\,Re)^{\frac{2}{15}} \quad \text{as} \quad Pr\,Ra\,Re \to \infty \tag{6.6}$$

and this gives practically the same result as (6.5) for $\epsilon = Pr\,Ra\,Re$ greater than 10^3.

7. Comparison with previous results

The heat transfer has been measured in horizontal pipes using water, air, and ethylene glycol. Different experimenters (followed by theoreticians) have plotted the Nusselt number versus a variety of dimensionless parameters, including *Ra*, *Re*, *Ra Re*, *Gr*, and *Gr Pr*, where the Grashof number *Gr* is (aside from possible factors of 2 in the definitions) equal to *Ra Re*/*Nu*. Anderson (1970) has criticized the last choice because both *Gr* and *Nu* contain the unknown average wall temperature. He emphasizes that the proper independent parameter is *Gr Nu Pr*, which is equivalent to our $\epsilon = Pr\,Ra\,Re$.

Anderson has converted to that parameter the measurements of Shannon & Depew (1968) in water, and the finite-difference calculations of Newell & Bergles (1970). Our figure 3, borrowed from Anderson, shows those results plotted versus our ϵ (rather than his $X^{\frac{1}{2}} = \epsilon/2$). We have added the measurements in air that Mori *et al.* (1966) originally plotted versus *Ra Re*.

Figure 3 shows that our result (6.6) agrees very well with the numerical solution and with the experiments for both air and water. Indeed, had we not been able to find the crucial exponent β from our series analysis, we could have estimated it from the experiments, using only our knowledge of the original radius of convergence ϵ_0. Thus figure 3 shows dotted curves for two alternate exponents, $\frac{1}{20}$ and $\frac{1}{10}$; and it is clear that the proper value must lie roughly halfway between them, as ours does.

Two different boundary-layer analyses have been proposed for the heated pipe. (Neither is a complete theory, however, because each is based on an assumption, suggested by experimental observations, about the structure of the flow in the core.) For Prandtl number not far away from unity, Mori & Futagami (1967) predict that the Nusselt number grows eventually as

$$\frac{Nu}{Nu_0} \sim C(Pr)\,(Ra\,Re)^{\frac{1}{5}}. \tag{7.1}$$

Their equations (48) and (56) show that the factor $C(Pr)$ is a complicated function of Prandtl number. For infinite Prandtl number, Siegwarth *et al.* (1969) predict that

$$Nu \sim 0.471\,(Gr\,Pr)^{\frac{1}{4}}, \tag{7.2}$$

and Cheng *et al.* (1972) and Woods & Morris (1980) point out that this can be converted to

$$\frac{Nu}{Nu_0} \sim 0.190\,(Pr\,Ra\,Re)^{\frac{1}{5}}. \tag{7.3}$$

However, both these results correspond to a value of $\frac{1}{10}$ for our exponent β; and that value was seen to be too large in figure 3. We conclude that the boundary-layer analyses are not correct.

8. Discussion

It is reassuring to find that our solution agrees with both experiment and numerical results over the entire range of laminar flow. Particularly gratifying is our ability to extract from the perturbation series for slight heating the asymptotic behaviour for extreme heating. It seems that the situation is more straightforward here than for the coiled pipe, where complete resolution of the paradox apparently awaits deeper understanding.

As Trefethen (1957) observed, the flow through a heated horizontal pipe is qualitatively similar in a number of respects to that through a coiled pipe or a rotating pipe. From a physical point of view, body forces produce in each case a double-spiral secondary motion. Transition to turbulence is thereby delayed to higher Reynolds numbers (for reasons that are by no means clear). From a mathematical point of view, the number of dimensionless parameters can in all three problems be reduced, to a good approximation, to a single combination: the Dean number for the coiled pipe, Mansour's product of axial and rotational Reynolds numbers for the rotating pipe, and Anderson's triple product $Pr\,Ra\,Re$ for the heated pipe. Expansion in powers of that single combination shows, in each case, convergence limited by a conjugate pair of square-root singularities on the imaginary axis. A global result was examined in each case, whose expansion involves only even powers, and is therefore limited by a square-root singularity on the negative axis.

Mapping that unphysical singularity away reveals a very weak singularity at infinity: a $\frac{1}{20}$-power for the coiled pipe, $\frac{1}{18}$ for the rotating pipe, and $\frac{1}{15}$ for our heated pipe. It is of no concern that these delicate estimates are different in each of the three cases, for the analogy is only qualitative. Each problem is quantitatively distinct; for example, our problem of the heated pipe involves a temperature equation that has no counterpart in the other two problems.

Another common feature is in each case an asymptotic result that contradicts existing boundary-layer analyses. For the loosely coiled pipe the friction grows eventually as the $\frac{1}{4}$-power of the 'practical' Dean number based on the actual mean flow speed down the pipe, rather than the $\frac{1}{2}$-power predicted by four different approximate boundary-layer models. For the rotating pipe, the friction grows as the $\frac{1}{8}$-power, rather than the $\frac{1}{4}$-power of two different boundary-layer approximations. And for the heated pipe we have found the heat transfer increasing as the $\frac{2}{15}$-power, not the $\frac{1}{5}$-power of the boundary-layer analyses of Mori & Futagami (1967) and Siegwarth *et al.* (1969).

The new experiments of Ramshankar & Sreenivasan seem to have substantiated our earlier conclusion (Van Dyke 1978) that the boundary-layer approximations for the coiled pipe are all not altogether correct. And the comparison shown in figure 3 convinces us that the boundary-layer results are also wrong for the heated pipe. Apparently we theoreticians do not yet fully understand how to treat a recirculating boundary layer – in particular, one that encloses a core of two bilaterally symmetric cells. Models have been invoked that assume collision of the layers from the two sides of the cross-section and subsequent formation of a re-entrant jet, or separation of the two layers before they meet, or layers that vanish just as they meet; but none of these has given correct results. We may hope that detailed local examination of computer-extended series solutions might elucidate the structure of recirculating boundary layers. That would undoubtedly require us to analyse local quantities, whereas we have so far considered only simpler global results.

Our approximation of high Prandtl number has proven not to be very restrictive. However, it would not be acceptable for a liquid metal like mercury, with $Pr = 0.02$. In that case the simplest approach would be to assume very small Prandtl number, corresponding to retention of only the first correction in Morton's approximation (2.7) rather than the third, because that would again involve a series in powers of only one parameter, $RaRe$. The more ambitious approach of treating arbitrary Prandtl number would require the analysis of double power series – a task for which we are not yet well equipped.

There are other fluid motions analogous to the three compared here. Thus Morris (1965) has calculated by hand the second-order solution in powers of rotational Rayleigh number for laminar flow through a heated vertical tube rotating about a parallel axis. It would be interesting to extend that series by computer, and compare it with the numerical and experimental results reported by Woods & Morris (1974, 1980).

We have discussed in detail only the first set of coefficients in table 1, with the boundary condition of zero conductivity and a Nusselt number referred to the bulk temperature. We now summarize our results for the other two sets, with infinite conductivity. Both show once more a square-root singularity on the negative axis of ϵ^2, but a common radius of convergence of $\epsilon_0 = 1996.356835$ rather than $1248.5\ldots$. The singularity at infinity has again an exponent of $\frac{1}{15}$ for Morton's Nusselt number based on mean temperature; but that is replaced by $\frac{2}{25}$ when Morton's result is recast

into bulk-temperature form. Thus the counterparts of our approximation (6.5) and its asymptotic form (6.6) are

$$\frac{Nu}{Nu_0} = \left[1 + \left(\frac{PrRaRe}{1996}\right)^2\right]^{\frac{1}{15}} \sim 0.3631\,(PrRaRe)^{\frac{2}{15}} \tag{8.1}$$

for Morton's version, and

$$\frac{Nu}{Nu_0} = \left[1 + \left(\frac{PrRaRe}{1996}\right)^2\right]^{\frac{2}{25}} \sim 0.2965\,(PrRaRe)^{\frac{4}{25}} \tag{8.2}$$

when referred to bulk temperature. The latter of these rises significantly faster than its zero-conductivity counterpart (6.6), but the difference is not great.

Bifurcation from a two-cell to a four-cell flow has been found numerically by Nandakumar, Masliyah & Law (1985) when Nu/Nu_0 has risen to about 2.4 (corresponding to the right side of our figure 3). Unfortunately the method of computer-extended series does not detect such a bifurcation, because it describes only the basic mode, which becomes unstable but continues analytically through the bifurcation point. It is conceivable that other solutions are described by our series on other Riemann sheets in the complex plane of ϵ, but we have no techniques yet for performing such an ambitious numerical analytic continuation.

This work was supported by the National Science Foundation under Grants ENG-7824412 and CTS-8821460. The author is indebted to Cliff Lin for the initial programming, and to A. J. Guttmann, William Reynolds, and Edward Sweeny for discussion and advice.

Appendix. The exponent at infinity

We have applied to our 16-term series a number of standard techniques (Gaunt & Guttmann 1974) in order to estimate the exponent of the singularity at infinity. We describe the three that yield the most conclusive results.

First, we examine the original series (5.1) using Padé approximants. Recall that the $[M/N]$ Padé approximant to a power series is the rational fraction

$$[M/N] = \frac{A_0 + A_1\epsilon + A_2\epsilon^2 + \ldots + A_M\epsilon^M}{1 + B_1\epsilon + B_2\epsilon^2 + \ldots + B_N\epsilon^N} \tag{A 1}$$

that, when expanded for small ϵ, matches the given series through ϵ^{M+N}. As the degrees M and N of the numerator and denominator both increase, Padé approximants provide analytic continuation far outside the original circle of convergence.

According to (6.3), the ratio Nu_0/Nu behaves like a multiple of $\epsilon^{-2\beta}$ as ϵ tends to infinity. Its logarithm therefore grows like $-2\beta\ln\epsilon$, and the derivative with respect to ϵ of the logarithm decays like $-2\beta/\epsilon$. We therefore calculate from (5.1) the series for the logarithmic derivative, and then form the successive Padé approximants $[N/(N+1)]$ with denominator of degree one greater than the numerator. As $\epsilon \to \infty$ these decay like $(A_N/B_{N+1})/\epsilon$ in the notation of (A 1), so that A_N/B_{N+1} provides an estimate of -2β. This gives the successive values

$$\beta = 0.0710,\quad 0.0772,\quad 0.0778,\quad 0.0778,\quad 0.0804,\quad 0.0682,\quad 0.0718. \tag{A 2}$$

It is characteristic of Padé approximants, as is the case here, that they do not vary smoothly even when applied to a smooth series. We can perhaps only conclude that β is 0.07 to one significant figure.

Second, we turn to the series (6.2) after the Euler transformation. If Nu_0/Nu is a multiple of $(1-\delta)^\beta$, its logarithmic derivative is

$$\frac{\mathrm{d}}{\mathrm{d}\delta}\ln\frac{Nu_0}{Nu} = \frac{-\beta}{1-\delta} = -\beta(1+\delta+\delta^2+\ldots+\delta^n+\ldots). \tag{A 3}$$

Thus the coefficients in the series for the logarithmic derivative provide the successive estimates

$$\begin{aligned}\beta = {} & 0.05745,\ 0.06841,\ 0.07272,\ 0.07486,\ 0.07605,\ 0.07675,\\ & 0.07716,\ 0.07740,\ 0.07754,\ 0.07760,\ 0.07761,\ 0.07759,\\ & 0.07755,\ 0.07749,\ 0.07742\end{aligned} \tag{A 4}$$

and these should approach the correct value. The last four values are decreasing smoothly, after having reached a maximum at the eleventh term. We can therefore extrapolate by forming a Neville table, which ends with

12	0.07151		
13	0.07104	0.07101	
14	0.07067	0.07060	0.07057
15	0.07035	0.07027	0.07022	0.07019

This table is again remarkably smooth, and the trend continually downward, suggesting that β is less than 0.070.

Experience shows that the values along the top diagonal of such a table can be extrapolated further. We apply to successive triads the nonlinear transformation

$$S = \frac{S_{n+1}S_{n-1}-S_n^2}{S_{n+1}+S_{n-1}-2S_n}, \tag{A 5}$$

which forms the exact sum S from any three successive partial sums S_n of a geometric sequence (Shanks 1955). It gives here the estimates

$$\begin{aligned}\beta = {} & 0.08280,\ 0.08135,\ 0.08694,\ 0.06436,\ 0.06883,\ 0.06912,\ 0.06894,\\ & 0.06871,\ 0.06840,\ 0.06816,\ 0.06795,\ 0.06775,\ 0.06758.\end{aligned} \tag{A 6}$$

From this we can perhaps conclude that β is 0.067 or 0.068 to two significant figures.

Third, we reconsider the Domb–Sykes plot for the Euler-transformed series. Although we have found it convenient to analyse the series for the reciprocal ratio Nu_0/Nu, it is helpful to examine also that for the direct ratio, which is found to be

$$\frac{Nu}{Nu_0} = 1+\sum_{n=1}^{\infty} d_n\,\delta^n = 1+0.05745\delta+0.03586\delta^2+0.02624\delta^3-\ldots. \tag{A 7}$$

We list the new coefficients d_n in table 2, and show in figure 2 the Domb–Sykes plot for this as well as the reciprocal series.

At first sight, figure 2 suggests a value of about $\beta = 0.1$ for both the direct and the reciprocal series. However, for large n the value for the direct series, at least, seems to be tending to somewhat smaller negative values. These graphical estimates are

refined by forming Neville tables for the exponent β. The end of a table biased to unit radius of convergence is, for the reciprocal series,

11...0.1191				
12...0.1159	0.1156			
13...0.1131	0.1126	0.1124		
14...0.1107	0.1101	0.1097	0.1094	
15...0.1086	0.1079	0.1073	0.1070	0.1068

and for the direct series

11...0.0236				
12...0.0252	0.0253			
13...0.0267	0.0270	0.0271		
14...0.0281	0.0285	0.0287	0.0288	
15...0.0294	0.0298	0.0302	0.0304	0.0305.

These two tables must have a common limit; but they are approaching it very slowly, so that we can only conclude that β lies between 0.03 and 0.10. However, we are free to modify the Domb–Sykes plot by renumbering the coefficients – for example, by setting $a_n = A_{n+1}$. This shifts the points in figure 2 considerably, so that those for the direct series lie practically on the line for $\beta = 0$. However, the points for the reciprocal series are then shifted by an almost equal amount. This suggests that a better estimate for β is given by the average of the values for the direct and the reciprocal series; and this idea is confirmed both by analysis and by examination of model functions. It is also equivalent to applying the 'critical-point renormalization' of Hunter & Baker (1973) to the direct and reciprocal series. Averaging the two tables above gives

11...0.07136				
12...0.07053	0.07046			
13...0.06990	0.06979	0.06973		
14...0.06941	0.06927	0.06919	0.06914	
15...0.06901	0.06886	0.06876	0.06869	0.06866.

We extrapolate further by applying the nonlinear transformation (A 5) to triads along the top diagonal. This gives the estimates

$$\beta = 0.09075,\ 0.09394,\ 0.09173,\ 0.08087,\ 0.12814,\ 0.07094,\ 0.06788,\ 0.06791,\ 0.06737,\ 0.06703,\ 0.06677,\ 0.06658,\ 0.06646 \qquad \text{(A 8)}$$

These values suggest that β is 0.066 or 0.067 to two figures.

REFERENCES

Anderson, A. D. 1970 Perturbation analysis of the quasi-developed flow of a liquid in a uniformly heated horizontal circular tube. Ph.D. dissertation, Stanford University. Univ. Microfilms order no. AAD71-12844.

Apostolakis, N. 1957 Effect of heat transfer upon flow field at low Reynolds numbers in horizontal tubes. M.S. thesis, University of Illinois, Urbana.

Barua, S. N. 1954 Secondary flow in a rotating straight pipe. *Proc. R. Soc. Lond.* A**227**, 133–139.

Batchelor, G. K. 1954 Heat transfer by free convection across a closed cavity between vertical boundaries at different temperatures. *Q. Appl. Maths* **21**, 209–233.

CHENG, K. C., HWANG, G. J. & AKIYAMA, M. 1972 On a simple correlation for Prandtl number effect on forced convective heat transfer with secondary flow. *Intl J. Heat Mass Transfer* **15**, 172–175.

COLLINS, W. M. & DENNIS, S. C. R. 1975 The steady motion of a viscous fluid in a curved tube. *Q. J. Mech. Appl. Maths* **28**, 133–156.

DASKOPOULOS, D. & LENHOFF, A. M. 1989 Flow in curved ducts: bifurcation structure for stationary ducts. *J. Fluid Mech.* **203**, 125–148.

DEAN, W. R. 1928 The stream-line motion of fluid in a curved pipe. *Phil. Mag.* **5**(7), 673–695.

DENNIS, S. C. R. 1980 Calculation of the steady flow through a curved tube using a new finite-difference method. *J. Fluid Mech.* **99**, 449–467.

GAUNT, D. S. & GUTTMANN, A. J. 1974 Series expansions: analysis of coefficients. In *Phase Transitions and Critical Phenomena* (ed. C. Domb & M. S. Green), vol. 3, pp. 181–243. Academic.

GILL, A. E. 1966 The boundary-layer regime for convection in a rectangular cavity. *J. Fluid Mech.* **26**, 515–536.

GOLDSTEIN, S. (ed.) 1938 *Modern Developments in Fluid Mechanics*. Oxford University Press.

HUNTER, C. 1987 Oscillations in the coefficients of power series. *SIAM J. Appl. Maths* **47**, 483–497.

HUNTER, D. L. & BAKER, G. A. 1973 Methods of series analysis. 1. Comparison of current methods used in the theory of critical phenomena. *Phys. Rev.* B7, 3346–3376.

IQBAL, M. & STACHIEWICZ, J. W. 1966 Influence of tube orientation on combined free and forced laminar convection heat transfer. *J. Heat Transfer* **88**, 109–116.

MANSOUR, K. 1985 Laminar flow through a slowly rotating straight pipe. *J. Fluid Mech.* **150**, 1–24.

MORCOS, S. M. & BERGLES, A. E. 1975 Experimental investigation of combined forced and free laminar convection in horizontal tubes. *J. Heat Transfer* **97**, 212–219.

MORI, Y. & FUTAGAMI, K. 1967 Forced convective heat transfer in uniformly heated horizontal tubes (2nd report, theoretical study). *Intl J. Heat Mass Transfer* **10**, 1801–1813.

MORI, Y., FUTAGAMI, K., TOKUDA, S. & NAKAMURA, M. 1966 Forced convective heat transfer in uniformly heated horizontal tubes. 1st report – experimental study on the effect of buoyancy. *Intl J. Heat Mass Transfer* **9**, 453–463.

MORRIS, W. D. 1965 Laminar convection in a heated vertical tube rotating about a parallel axis. *J. Fluid Mech.* **21**, 453–464.

MORTON, B. R. 1959 Laminar convection in uniformly heated horizontal pipes at low Rayleigh number. *Q. J. Mech. Appl. Maths* **12**, 410–420.

NANDAKUMAR, K., MASLIYAH, J. H. & LAW, H. S. 1985 Bifurcation in steady laminar mixed convection flow in horizontal ducts. *J. Fluid Mech.* **152**, 145–161.

NEWELL, P. H. & BERGLES, A. E. 1970 Analysis of combined free and forced convection for fully developed laminar flow in horizontal tubes. *J. Heat Transfer* **92**, 83–93.

NUSSELT, W. 1910 Die Abhängigkeit der Wärmeübergangszahl von der Rohrlänge. *Z. Vereines Deutscher Ing.* **54**, 1154–1158.

RAMSHANKAR, R. & SREENIVASAN, K. R. 1988 A paradox concerning the extended Stokes series solution for the pressure drop in coiled pipes. *Phys. Fluids* **31**, 1339–1347.

REYNOLDS, W. C. & POTTER, M. C. 1967 Finite-amplitude instability of parallel shear flows. *J. Fluid Mech.* **27**, 465–492.

SHANKS, D. 1955 Non-linear transformations of divergent and slowly convergent sequences. *J. Maths & Phys.* **34**, 1–42.

SHANNON, R. L. & DEPEW, C. A. 1968 Combined free and forced laminar conduction in a horizontal tube with uniform heat flux. *J. Heat Transfer* **90**, 353–357.

SIEGWARTH, D. P., MIKESELL, R. D., READAL, T. C. & HANRATTY, T. J. 1969 Effect of secondary flow on the temperature field and primary flow in a heated horizontal tube. *Intl J. Heat Mass Transfer* **12**, 1535–1552.

TREFETHEN, L. 1957 Fluid flow in radial rotating tubes. *Actes 9ème Congr. Intle. Méc. Appl.* vol. 1, pp. 341–350. University of Bruxelles.

VAN DYKE, M. 1970 Extension of Goldstein's series for the Oseen drag of a sphere. *J. Fluid Mech.* **44**, 365–372.

VAN DYKE, M. 1978 Extended Stokes series: laminar flow through a loosely coiled pipe. *J. Fluid Mech.* **86**, 129–145.

WOODS, J. L. & MORRIS, W. D. 1974 An investigation of laminar flow in the rotor windings of directly-cooled electrical machines. *J. Mech. Engng Sci.* **16**, 408–417.

WOODS, J. L. & MORRIS, W. D. 1980 A study of heat transfer in a rotating cylindrical tube. *J. Heat Transfer* **102**, 612–616.